Molecular Biology of the Cell
Vol. 15, 2884–2894, June 2004

Role of Cytoplasmic Domain Serines in Intracellular Trafficking of Furin

Florencia B. Schapiro, Thwe Thwe Soe, William G. Mallet, and Frederick R. Maxfield*

Department of Biochemistry, Weill Medical College of Cornell University, New York, New York 10021

Submitted September 9, 2003; Revised March 23, 2004; Accepted March 26, 2004
Monitoring Editor: Jean Gruenberg

Furin is a transmembrane protein that cycles between the plasma membrane, endosomes, and the *trans*-Golgi network, maintaining a predominant distribution in the latter. It has been shown previously that Tac-furin, a chimeric protein expressing the extracellular and transmembrane domains of the interleukin-2 receptor α chain (Tac) and the cytoplasmic domain of furin, is delivered from the plasma membrane to the TGN through late endosomes, bypassing the endocytic recycling compartment. Tac-furin also recycles in a loop between the TGN and late endosomes. Localization of furin to the TGN is modulated by a six-amino acid acidic cluster that contains two phosphorylatable serines (SDSEED). We investigated the role of these serines in the trafficking of Tac-furin by using a mutant chimera in which the SDS sequence was replaced by the nonphosphorylatable sequence ADA (Tac-furin/ADA). Although the mutant construct is internalized and delivered to the TGN, both the postendocytic trafficking and the steady-state distribution were found to differ from the wild-type. In contrast with Tac-furin, Tac-furin/ADA does not enter late endosomes after being internalized. Instead, it traffics with transferrin to the endocytic recycling compartment, and from there it is delivered to the TGN. As with Tac-furin, Tac-furin/ADA is sorted from the TGN into late endosomes at steady state, but its retrieval from the late endosomes to the TGN is inhibited. These results suggest that serine phosphorylation plays an important role in at least two steps of Tac-furin trafficking, acting as an active sorting signal that mediates the selective sorting of Tac-furin into late endosomes after internalization, as well as its retrieval from late endosomes back to the TGN.

INTRODUCTION

The transport of proteins to the appropriate subcellular destinations is a critical aspect of cellular homeostasis and also plays a major role in the interaction of cells with their environment. Membrane proteins are transferred among cellular organelles by using a variety of membrane transport pathways (Mukherjee *et al*., 1997; Gu *et al*., 2001; Maxfield and McGraw, 2004). Although many transport routes are specific to the biosynthetic or endocytic systems, these two major trafficking routes have several points of intersection. Most notably, a group of membrane proteins are internalized from the plasma membrane and delivered to the *trans*-Golgi network (TGN), rather than following the predominant recycling or degradative pathways. Among these proteins are the cation-independent mannose 6-phosphate/insulin-like growth factor II receptor (Duncan and Kornfeld, 1988), metallocarboxypeptidase D (Varlamov *et al*., 1999), peptidylglycine-amidating monooxygenase (Milgram *et al*., 1993), furin (Bosshart *et al*., 1994; Molloy *et al*., 1994; Schafer *et al*., 1995; Takahashi *et al*., 1995), and TGN38 (Bos *et al*., 1993; Jones *et al*., 1993; Reaves *et al*., 1993).

The transport to the TGN of chimeric forms of two of these membrane proteins, furin and TGN38, has been investigated in the Chinese hamster ovary (CHO)-derived TRVb-1 cell line (Ghosh *et al*., 1998; Mallet and Maxfield, 1999). The chimeras used in these studies comprised the cytoplasmic domain of furin or TGN38 and the transmembrane and lumenal domains of the interleukin-2 receptor α chain (Tac) (Bosshart *et al*., 1994). These constructs allowed analysis of postendocytic transport by binding labeled anti-Tac monoclonal antibodies at the surface and then following the fates of the internalized antibodies. Tac-TGN38 and Tac-furin were found to be targeted from the plasma membrane to the TGN via two independent pathways: whereas Tac-TGN38 enters the endocytic recycling compartment (ERC) and is delivered to the TGN by iterative removal from the recycling pathway, Tac-furin completely evades this route, neither occurring in the ERC nor rapidly returning to the plasma membrane. In contrast with Tac-TGN38, transport of Tac-furin to the TGN is mediated by late endosomes, through an efficient, single-pass mechanism. Despite the differences in the transport routes and the sorting mechanisms, both Tac-TGN38 and Tac-furin localize predominantly to the TGN at steady state, mainly due to their relatively low net rates of return to the plasma membrane from this organelle (Mallet and Maxfield, 1999).

Segregation of TGN38 from the bulk of internalized membrane proteins that traverse the recycling pathway requires selective sorting based on protein–protein interactions or selective partitioning into membrane domains based on physical properties. The mechanisms involved in this sorting process have not been fully elucidated. A cytoplasmic sequence, SDYQRL, has been found to be essential for routing of TGN38 to the TGN (Bos *et al*., 1993; Humphrey *et al*., 1993), but this sequence is not sufficient for delivery of other molecules from the ERC to the TGN (Johnson *et al*., 1996), suggesting that other cytoplasmic and/or transmembrane sequences, yet unidentified, are required for targeting of TGN38 to the TGN.

Article published online ahead of print. Mol. Biol. Cell 10.1091/mbc.E03–09–0653. Article and publication date are available at www.molbiolcell.org/cgi/doi/10.1091/mbc.E03–09–0653.

* Corresponding author. E-mail address: frmaxfie@med.cornell.edu.

Sorting of furin has been shown to depend on defined sequence motifs within its 56-amino acid cytoplasmic domain. The characterized sorting signals include the tyrosine-based motif YKGL[765], involved in internalization from the plasma membrane and sorting from the TGN, and the acidic cluster EECPSDSEEDEG[780], required for TGN localization (Schafer *et al*., 1995; Takahashi *et al*., 1995; Voorhees *et al*., 1995). The serine residues at position 773 and 775 of this acidic cluster are phosphorylated by casein kinase II (CKII) and dephosphorylated by protein phosphatase 2A (PP2A) in vitro and in vivo (Jones *et al*., 1995; Molloy *et al*., 1998). These observations led to a model of furin trafficking, which comprises two local cycling loops: one between the cell surface and sorting endosomes, and the other between the TGN and a late endosomal compartment. According to this model, cell surface furin is endocytosed in a clathrin-dependent step by direct interaction of the tyrosine internalization motif with the AP-2 adaptor (Schafer *et al*., 1995). Once in sorting endosomes, furin has been reported to undergo a phosphorylation-dependent sorting step that is controlled by the activities of CKII and PP2A (Jones *et al*., 1995; Molloy *et al*., 1998). It has been suggested that CKII-phosphorylated furin molecules bind the connector protein phosphofurin acidic cluster sorting protein 1 (PACS-1), which links them to the sorting machinery, placing them in a local cycling loop between the sorting endosomes and the cell surface (Molloy *et al*., 1998). In contrast, furin molecules dephosphorylated by PP2A are proposed to exit the plasma membrane/sorting endosomes cycling loop and enter the TGN (Molloy *et al*., 1998). The role of serine phosphorylation in further transport steps to the TGN has not been completely elucidated. The second cycling loop comprises sorting of furin from the TGN into a late endosomal compartment by binding of a tyrosine-based motif to the clathrin-associated adaptor AP-1 (Wan *et al*., 1998). Retrieval to the TGN has been proposed to be mediated by PACS-1, which links phosphofurin to the clathrin-associated adaptor, AP-1 (Wan *et al*., 1998).

In the present work, we further analyzed the involvement of the phosphorylatable serines in the postendocytic trafficking of Tac-furin using a well-characterized CHO cell line, TRVb-1 (McGraw *et al*., 1987). The trafficking of mutant constructs, in which the SDS sequence of the acidic cluster was replaced by the nonphosphorylatable sequence ADA, was followed by incubating live cells with fluorescently labeled monoclonal antibodies against the Tac ectodomain. Our results indicate that the serine residues of the acidic cluster of Tac-furin are involved in at least two different steps of the transport of this protein. Neither internalization nor TGN-targeting of Tac-furin was found to depend on the phosphorylatable serines. However, the substitution of these residues by alanines changes the route by which Tac-furin is delivered to the TGN after internalization: instead of going through late endosomes, as seen for wild-type (WT) Tac-furin, targeting of Tac-furin/ADA involves passage through the ERC. The mutation also slows the retrieval from late endosomes back to the TGN.

MATERIALS AND METHODS

Cells and Constructs

Chimeric Tac-furin protein constructs TTF in the plasmid pCDM8.1 incorporating the cytomegalovirus promoter were obtained from Michael Marks (University of Pennsylvania, Philadelphia, PA) (Bosshart *et al*., 1994). TTF/ADA constructs were created with QuikChange site-directed mutagenesis (Stratagene, La Jolla, CA), by using the 5′ primer 5′-GAG GAG TGC CCA GCG GAC GCA GAG GAG GAC G and the 3′ primer 5′-CGT CCT CCT CTG CGT CCG CTG GGC ACT CCT C. Primers were purchased from Invitrogen (Carlsbad, CA). TRVb-1 cells, a CHO cell line that lacks endogenous transferrin receptors but stably expresses the human transferrin receptor (McGraw *et al*., 1987), were cotransfected with either the wild-type or ADA mutant Tac-furin plasmids and the pMEP plasmid (encoding resistance to hygromycin) by using the LipofectAMINE reagent system (Invitrogen). Cells expressing the constructs were selected by culturing in Ham's F-12 medium containing 200 U/ml hygromycin B, 100 μg/ml penicillin-streptomycin, 400 μg/ml G418, 5% fetal bovine serum and 220 mM sodium bicarbonate at 37°C in a humidified atmosphere of 5% CO_2. To isolate clonal lines stably expressing similar levels of the wild-type and mutant chimeric constructs, cells were incubated with Ax488-anti-Tac IgG at 37°C for 60–120 min to allow labeling to steady state. Cells were sorted by fluorescence-activated cell sorting, and single cell colonies with similar levels of expression were grown. All data were derived from monoclonal populations, and qualitatively similar behavior was observed in mixed colonies of cells.

Antibodies and Fluorescent Reagents

Monoclonal antibodies (IgG1) against the Tac epitope were purified from ascites fluid prepared from the hybridoma cell line 2A3A1H (American Type Culture Collection, Manassas, VA) by using protein G affinity chromatography. Antibodies were conjugated to Alexa 488 (Ax488-anti-Tac; Molecular Probes, Eugene, OR) or Alexa 546 (Ax546-anti-Tac), according to the manufacturer's instructions. Low-density lipoproteins (LDLs) labeled with 1,1′-dioctadecyl-3,3,3′,3′-tetramethylindocarbocianine $(DiI)_{16}$ were prepared as described previously (Pitas *et al*., 1981). Fixable 70-kDa dextrans conjugated to rhodamine and Ax546-goat anti-rabbit IgG were purchased from Molecular Probes. Polyclonal antibodies against the cytoplasmic domain of rat TGN38 were a kind gift of Dr. George Banting (University of Bristol, Bristol, United Kingdom).

Fluorescence Staining Methods

For microscopy, cells were plated onto poly-D-lysine–treated no. 1 coverslips affixed beneath holes cut into the bottoms of 35-mm tissue culture dishes. Experiments were performed 2 d after plating the cells. Live cells were incubated for the specified time with Ax488 or Ax546-anti-Tac IgG (3 μg/ml) in McCoy's 5A medium (Invitrogen) supplemented with 0.2% (wt/vol) bovine serum albumin (BSA) (Sigma-Aldrich, St. Louis, MO), 2.2 g/l $NaHCO_3$, and 20 mM HEPES (McCoy's modified medium). Cells were then washed with medium 1 (150 mM NaCl, 20 mM HEPES, 1 mM $CaCl_2$, 5 mM KCl, 1 mM $MgCl_2$, pH 7.4) and chased for the indicated periods of time in McCoy's modified medium. All incubations were performed at 37°C. Unless noted, cells were then fixed with 4% paraformaldehyde in PBS. For indirect immunofluorescence labeling, fixed cells were permeabilized with 0.01% (wt/vol) saponin (Sigma-Aldrich) in medium 1. Cells were then incubated for 30 min in medium 1 with 0.01% (wt/vol) saponin and 0.5% (wt/vol) BSA to avoid nonspecific binding, washed, and incubated with anti-TGN38 (6 μg/ml) for an hour. After the primary antibody incubation, cells were washed and incubated with Ax546-goat anti-rabbit IgG (8 μg/ml) for another hour. All incubations were performed at room temperature.

Microscopy

Confocal microscopy was performed using an LSM 510 laser scanning unit (Carl Zeiss, Thornwood, NY) on an Axiovert 100M inverted microscope (Carl Zeiss) with a 63× 1.4 numerical aperture plan Apochromat objective (Carl Zeiss). Excitation was with a 25-mW argon laser emitting at 488 nm, a 1.0-mW helium/neon laser emitting at 543 nm, and a 5.0-mW helium/neon laser emitting at 633 nm. Emissions were collected using a 505–530-nm band pass filter to collect Ax488 emissions and a 560- to 615-nm band pass filter to collect Ax546 and DiI emissions. Typically, 0.5-μm vertical steps were used, with a vertical optical resolution of $<$1.0 μm. Cross talk of the fluorophores was negligible.

Cellular Accumulation of ^{125}I-Anti-Tac Antibody

Cells grown to confluence on 24-well plates were incubated with ^{125}I-anti-Tac antibody in McCoy's 5A modified medium (final IgG concentration of 10 μg/ml) for 5, 15, 30, 60, 120, and 180 min at 37°C. At the end of each incubation, cells were washed extensively with ice-cold medium 1 with 1% (wt/vol) BSA and were solubilized in 0.1% (wt/vol) SDS in 0.1 M NaOH. Solubilized radioactivity corresponding to each time point was determined using a gamma counter. Nonspecific counts were determined by conducting parallel experiments on untransfected TRVb-1 cells and were subtracted from the counts extracted from cells. In each experiment, triplicate wells were used for each time point.

Nocodazole Studies

Cells were labeled with Ax456-anti-Tac (15-min chase, 2-h pulse), followed by an incubation in nocodazole (33 μM) for 30 min at 4°C and then for another 30 min at 37°C. Nocodazole-treated cells were fixed, permeabilized, and stained with anti-TGN38, as described above. A separate control experiment was performed, in which cells received 0.1% (vol/vol) dimethyl sulfoxide to control for effects of the solvent in which nocodazole is dissolved.

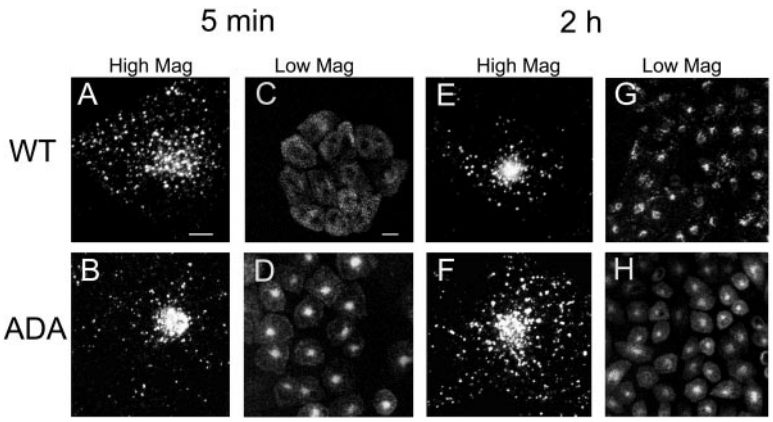

Figure 1. Postendocytic and steady-state distribution of Tac-furin and Tac-furin/ADA in TRVb-1 cells. Cells expressing either the Tac-furin or the Tac-furin/ADA construct (ADA) were incubated for 5 min with Ax546–anti-Tac antibodies, washed and chased for 5 min (A–D) or 2 h (E–H) before fixation. Confocal projections obtained at a high (A, B, E and F) and low (C, D, G, and H) magnification are shown. Bar (A, B, E, and F), 10 μm. Bar (C, D, G, and H), 5 μm.

Fluorescence Ablation with Horseradish Peroxidase-Transferrin (HRP-Tf) or HRP

HRP-Tf was prepared as described by Ghosh *et al.* (1998). Cells were incubated with 50 μg/ml HRP-Tf and either 5 μg/ml Ax488-Tf or 8 μg/ml Ax488-anti-Tac IgG (pulse) and then chased in the presence of 50 μg/ml HRP-Tf. Pulse and chase incubations were performed in McCoy's modified medium at 37°C for the indicated periods of time. Late endosomes were labeled by preincubating cells with 2 mg/ml HRP (Sigma-Aldrich) for 15 min at 37°C. Cells were then washed and labeled with 8 μg/ml Ax488-anti-Tac for 5 min, after a 10-min chase. At the end of the respective chases, cells were placed on ice, washed with cold medium 1, and either incubated with 0.0025% hydrogen peroxide and 25 μg/ml diaminobenzidine (DAB) or in medium 1 (control) for 2 h. After the hydrogen peroxide/DAB treatment cells were washed with Medium 1 and fixed before viewing on the microscope. The cell-associated fluorescence intensity in control and treated cells was quantified using MetaMorph software. All images were corrected for background fluorescence. The extent of HRP-mediated quenching was expressed as the percentage of total fluorescence intensity in control cells. The efficiency of the HRP ablation was independently confirmed by testing quenching of internalized Ax488-Tf and fluorescein isothiocyanate (FITC)-dextran.

Photobleaching

Live cells were incubated for 5 min with Ax488–anti-Tac, washed, and chased for 2 h. Images recording the initial fluorescence were acquired, followed by the selective bleaching of the labeled Golgi complex on the LSM 510 laser confocal microscope by scanning the selected region with high intensity illumination (100% transmittance). Images were acquired right after bleaching, and the recovery of fluorescence monitored at 2, 5, 15, 30, and 45 min thereafter. Cell-associated fluorescence intensity (F_T) and fluorescence intensity of the bleached area (F_G) at the different time points on single optical sections were quantified using MetaMorph (Universal Imaging, Downingtown, PA) and plotted as F_G/F_T versus time. All images were corrected for background fluorescence.

Quenching Studies

To assess recycling at short times after internalization, cells were incubated with Ax488-anti-Tac for 5 min, washed, and chased for 2, 5, 15, and 30 min in the presence of the quenching antibody anti-Ax488 (100 μg/ml). To investigate the retrieval of the constructs from the TGN back to the cell surface at steady state, cells were pulsed for 30 min, chased for 2 h, and further incubated in the presence of the quenching antibody for 5, 15, 30, 60, 90, and 120 min. In both experiments, after the chase cells were fixed and the fluorescence intensity quantified.

Image Processing and Quantification

Processing of digitized images was performed using the MetaMorph image processing software package (Universal Imaging). All images were corrected for background fluorescence. To quantify fluorescence intensity per cell (Fluo/Cell), the background fluorescence value was subtracted from images, and the remaining fluorescence power in the field was summed and divided by the number of cells in the field; typically, 10 fields of ~20 cells per field were analyzed for each data point in a single experiment.

Lifetime Measurements

Cells grown to confluence were labeled overnight at 37°C with 0.1 mCi/ml [^{35}S]methionine and [^{35}S]cysteine (PerkinElmer Life and Analytical Sciences, Boston, MA), washed, and chased in growth medium supplemented with 10× methionine/cysteine (Sigma-Aldrich) for 0, 1.5, 3, 6, 12, and 24 h. Cells were lysed in lysis buffer (20 mM Tris-HCl, pH 8, 150 mM NaCl, 0.2% BSA, 5 mM

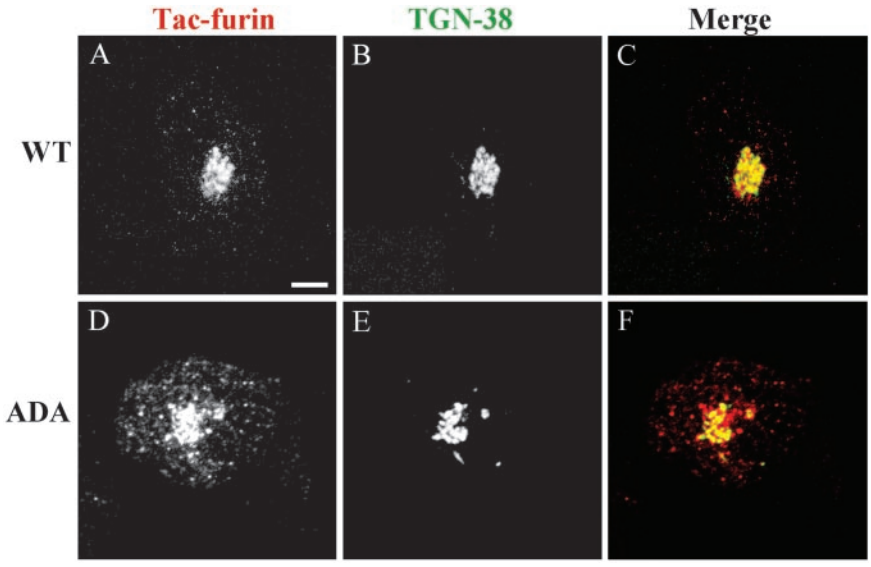

Figure 2. Tac-furin/ADA localizes to the TGN at steady state. Cells were incubated for 5 min with Ax546–anti-Tac (A and D), washed, and chased for 2 h. Cells were then fixed, permeabilized, and labeled with polyclonal antibodies against TGN-38, followed by Ax488–anti-rabbit antibodies (B and E). (C and F) Merge of the anti-Tac signal (red) and the TGN38 signal (green). Colocalized areas range from orange to yellow. Single confocal planes are shown. Bar, 10 μm.

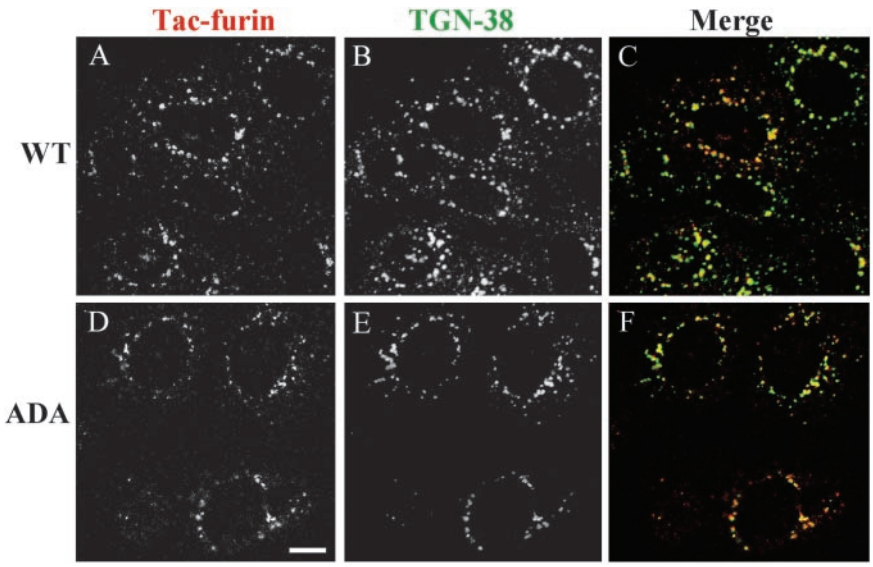

Figure 3. Tac-furin/ADA localizes to TGN fragments after nocodazole treatment. Cells were labeled for 15 min with Ax546–anti-Tac (A and D), washed, and chased for 2 h. Labeled cells were incubated with nocodazole (33 μM) at 4°C for 30 min and then for another 30 min at 37°C, fixed, permeabilized and stained with anti-TGN38, as described in Figure 2 (B and E). C and F show the merge of the anti-Tac signal (red) and the TGN38 signal (green). Colocalized areas range from orange to yellow. Single confocal planes are shown. Bar, 10 μm.

EDTA, 1%Triton X-100, 2 mM 4-(2-aminoethyl)benzenesulfonyl fluoride, 10 μg/ml each leupeptin, pepstatin, and aprotinin [Sigma-Aldrich]), preadsorbed on pansorbin (Calbiochem, San Diego, CA), and immunoprecipitated with 2 μg/ml anti Tac-antibody followed by 2 μg/ml rabbit anti-mouse IgG. Immunocomplexes were collected on protein A-agarose and eluted in SDS-PAGE buffer. Samples were separated on 10% PAGE gels; gels were exposed on PhosphorImager screens, and the radioactivity was quantified with the IQMac-program of Amersham Biosciences (Piscataway, NJ).

RESULTS

Time Course of Tac-Furin and Tac-Furin/ADA Trafficking in TRVb-1 Cells

The postendocytic trafficking of the WT and ADA mutant forms of Tac-furin was compared in stable transfectants of the CHO-derived TRVb-1 cell line. Cells were incubated in the presence of Ax546-anti-Tac antibodies for 5 min at 37°C, and then washed and chased for 5, or 120 min before fixation. As shown in Figure 1, although Tac-furin/ADA is internalized rapidly, its subcellular distribution differs from that of the wild type (WT), both at early times after internalization and at steady state. Corroborating previous observations (Mallet and Maxfield, 1999), after a 5-min chase, internalized Tac-furin exhibits a punctate distribution throughout the cell consistent with localization in early sorting endosomes (Figure 1, A and C). In contrast, the ADA mutant is primarily detected in a tight central compartment with only a small fraction found in peripheral vesicles (Figure 1, B and D). The steady-state distribution of the two constructs also differs. After a 2-h chase, Tac-furin localizes mostly to a juxtanuclear compartment, with a small fraction present in peripheral vesicles (Figure 1, E and G). Although the Tac-furin/ADA is present in a juxtanuclear compartment as well, it also displays an abundant vesicular staining throughout the cytoplasm (Figure 1, F and H). These results show that substitution of the phosphorylatable serines affects the intracellular routing of Tac-furin. A small fraction of the internalized antibody was degraded in both cell lines (our unpublished data), indicating that the mutant Tac-furin is not mistargeted for degradation.

At Steady State, Tac-Furin/ADA Localizes to the TGN and a Late Endosomal Compartment

As shown in Figure 1F, Tac-furin/ADA localizes to a juxtanuclear compartment at steady state. To assess whether this construct is targeted to the TGN, we compared the distribution of antibody-labeled Tac-furin/ADA with endogenous TGN38 detected by immunofluorescence. Cells

Table 1. Assessment of Ax488-labeled Tac-furin and Tac-furin/ADA distribution by fluorescence ablation

	Fluorescence ablation (% ± SE)		
	Steady state	Postendocytic quenching by HRP-Tf	Postendocytic quenching by HRP
Cell Line	Pulse: Ax488 anti-Tac, 5 min Chase: HRP-Tf, 2 h	Pulse: Ax488 anti-Tac, 5 min Chase: HRP-Tf, 10 min	Preincubation: HRP, 15 min Pulse: Ax488-anti-Tac, 5 min Chase: HRP, 10 min
WT	12 ± 2	20 ± 4	64 ± 8
ADA	15 ± 3	72 ± 10	15 ± 2

Cells were pulsed with Ax488-anti-Tac antibody, washed, and chased in the presence of HRP-Tf or HRP for the indicated times. At the end of the chases, cells were placed on ice and incubated with H_2O_2 and DAB or medium 1 (control). The extent of DAB-mediated fluorescence ablation is expressed as the percentage of total fluorescence intensity of control cells. For comparison, quenching of Ax488-Tf by HRP-Tf was 77–80%.

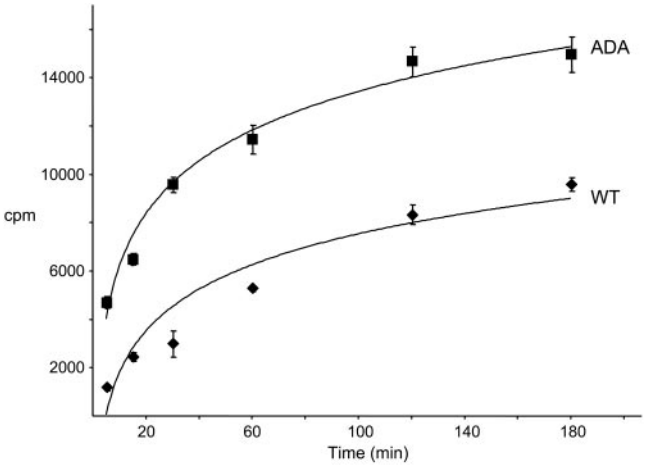

Figure 4. Accumulation of ^{125}I-anti-Tac antibody in WT and ADA mutant cell lines. Cells were incubated with ^{125}I-anti-Tac antibody for 5, 15, 30, 60, 120, or 180 min at 37°C, washed extensively with ice-cold medium 1 with 1% (wt/vol) BSA, and solubilized. Cell-associated radioactivity corresponding to each time point was measured. Error bars represent SEM.

were incubated with Ax546–anti-Tac antibody for 5 min, washed, and chased for 2 h to achieve a steady-state distribution. Cells were then fixed and stained for TGN38. As a control, the distribution of Tac-furin also was evaluated by immunofluorescence with anti-Tac antibody. Preliminary control experiments showed that the anti-Tac staining in fixed, permeabilized cells is similar to that obtained after a prolonged chase (2 h) of the antibody in both WT and mutant live cell lines, indicating that anti-Tac does not alter the distribution of Tac-furin (our unpublished data).

Confirming previous observations (Mallet and Maxfield, 1999), endocytosed Tac-furin colocalizes with TGN38 in the TGN (Figure 2, A–C). Colocalization between Tac-furin/ADA and TGN38 also was observed (Figure 2, D–F), indicating that a portion of the mutant construct is delivered to the TGN after internalization. Nocodazole treatment leads to the dispersal of Golgi elements, providing an additional means to verify the distribution of Tac-furin/ADA. As shown in Figure 3, partial colocalization of both the ADA mutant (D–F) and WT (A–C) constructs with TGN38 persists in nocodazole-treated cells. Please note that Figure 1 shows confocal projection images, whereas Figures 2 and 3 show single confocal planes corresponding to the brightest TGN38 labeling.

To assess whether a portion of the mutant construct is present as well in the ERC at steady state, we used an HRP fluorescence ablation technique that extinguishes the fluorescence from any fluorescent probe that is in the same compartment as HRP (Mayor *et al.*, 1998). A positive control to confirm that Ax488-Tf fluorescence can be quenched using HRP-Tf was performed by incubating cells with Ax488-Tf for 30 min, chasing for 10 min with HRP-Tf, and treating with hydrogen peroxide and DAB or incubating with medium 1. The Ax488 fluorescence observed in control cells is significantly quenched in treated cells. Quantification of the fluorescence intensity per cell of control and treated cells shows that the DAB quenches 77 and 80% of the Ax488-Tf fluorescence in WT and mutant cells, respectively. To allow labeling of Tac-furin to steady state, cells were incubated with Ax488-anti-Tac IgG for 5 min and then chased for 2 h. HRP-Tf was present in the medium during the last hour of the chase. The fluorescence of WT and ADA mutant cells were quenched by 12 and 15%, respectively (Table 1), indicating that there is relatively little of the constructs in transferrin-containing organelles at steady state.

We measured the rate of accumulation of anti-Tac antibodies in WT and mutant cell lines. Cells were incubated with ^{125}I-anti-Tac at 37°C for increasing lengths of time, and the cell-associated radioactivity for each time point was measured. The approach to steady-state labeling of both cell lines can be described by a single first-order process with a half-time of ~34 min for the WT, corroborating previous results (Mallet and Maxfield, 1999), and ~25 min for the ADA mutant cell lines (Figure 4). There may have actually been more than one underlying rate constant, but these data could be fit with a single rate constant. The steady-state values indicate that expression of the Tac-furin/ADA was ~60% higher than expression of the wild-type construct.

A portion of Tac-furin and Tac-furin/ADA is also present in punctate, vesicular structures throughout the cytoplasm at steady state (Figure 1, C and F). This cytoplasmic staining is clearly more abundant in Tac-furin/ADA-expressing cells than in WT cells. Taking into consideration previous studies, which suggest that at steady-state furin cycles between the TGN and a late endosomal compartment (Molloy *et al.*, 1999; Mallet and Maxfield, 1999), we labeled the late endosomal compartments by preincubating cells for 6 h with FITC-dextran and then incubated cells with Ax546-anti-Tac antibody (5-min pulse, 2-h chase, with FITC-dextran present in the chase medium for the first hour). As shown in Figure 5,

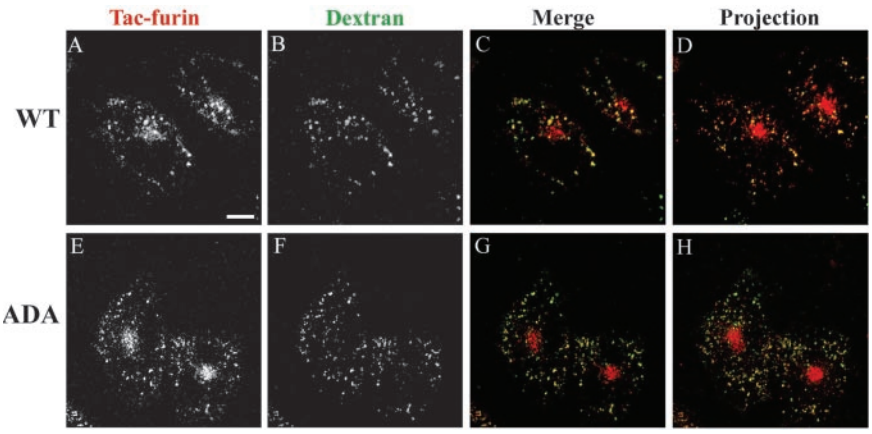

Figure 5. Tac-furin/ADA is sorted into late endosomes at steady state. Late endosomes were labeled by preincubating cells with FITC-dextran (B and F) for 6 h. Cells were then washed, pulsed with Ax546–anti-Tac (A and E) for 5 min, and chased for 2 h before fixation. FITC-dextran was present in the medium throughout the pulse and the first hour of the chase. (C and G) Merge of the anti-Tac signal (red) and the dextran signal (green). A–C and E–G show single confocal planes. A projection of successive confocal planes is shown in D and H. Colocalized areas range from orange to yellow. Bar, 10 μm.

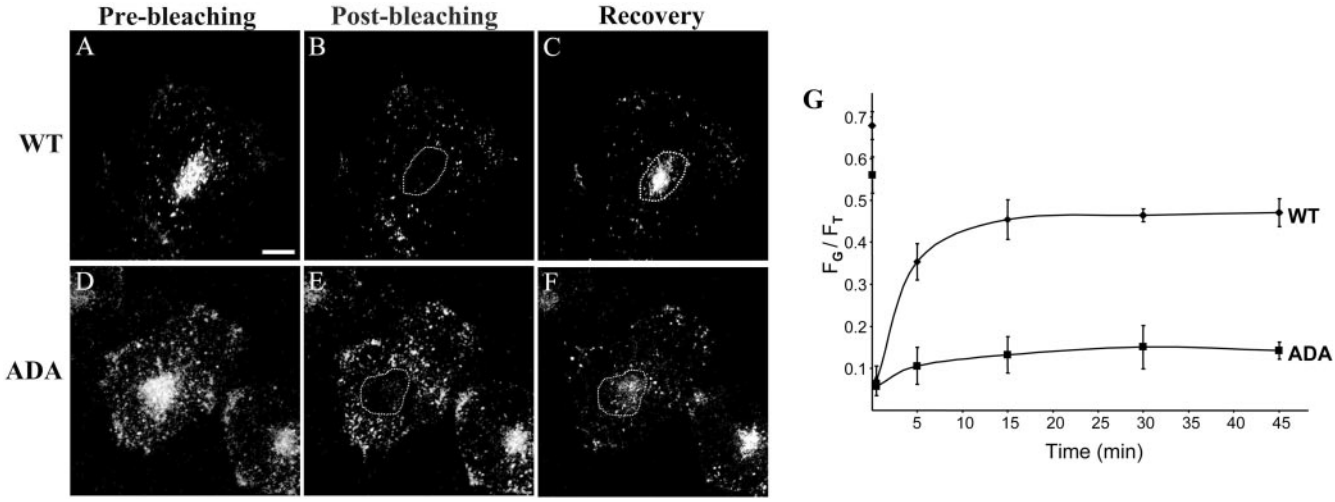

Figure 6. Retrieval of Tac-furin/ADA from late endosomes back to the TGN at steady state is significantly inhibited. Cells were incubated for 5 min with Ax488–anti-Tac, washed, and chased for 2 h. Selective bleaching of the Golgi complex of labeled cells was then performed on a LSM 510 by scanning with high-intensity illumination (100% transmittance). The recovery of fluorescence in the bleached region was monitored at 2, 5, 15, 30, and 45 min thereafter. A–F. Single confocal planes showing the fluorescence distribution immediately before bleaching (prebleaching, A and D), immediately after bleaching (postbleaching, B and E) and 45 min after bleaching (recovery, C and F). Bar, 10 μm. (G) Kinetics of Tac-furin/ADA retrieval from late endosomes back to the TGN at steady state. For the imaged focal plane, total cell-associated fluorescence (F_T) and fluorescence of the bleached area (F_G) at the different time points were quantified and plotted as F_G/F_T versus time. Also represented are the levels of Tac-furin and Tac-furin/ADA fluorescence that localized to the Golgi within the selected focal plane before photobleaching. Data points represent the means of two independent experiments. Error bars represent SEM.

the punctate structures containing the furin construct and late endosomes labeled by FITC-dextran present a very good codistribution, both in WT and ADA mutant cell lines.

Retrieval of Tac-Furin/ADA from Late Endosomes to the TGN at Steady State Is Strongly Inhibited

To investigate whether the altered steady-state distribution of Tac-furin/ADA is due to slower return to the TGN from late endosomes, we selectively photobleached the Golgi region of cells labeled with Ax488-anti-Tac and monitored the recovery of fluorescence in the bleached region (Figure 6, A–F). Before photobleaching, the percentage of Tac-furin/ADA fluorescence that localized to the Golgi within the selected focal plane, which contained the Golgi apparatus, was 68 and 57%, for WT and ADA mutant cell lines, respectively (Figure 6 G). Within 45 min after photobleaching, the Golgi complex of the WT cell line regained 46% of the cellular fluorescence (Figure 6G, diamonds). In contrast, only 11% of the cellular fluorescence was retrieved to the Golgi region in the ADA mutant cell line (Figure 6G, squares). These results show that retrieval of Tac-furin/ADA from late endosomes back to the TGN at steady state is significantly inhibited, accounting for the abundant punctate pattern observed for the Tac-furin/ADA at steady state.

Tac-Furin/ADA Is Targeted to the TGN through the ERC, without Initial Delivery into Late Endosomes

Internalized Tac-furin is targeted to the TGN through late endosomes, bypassing the ERC (Mallet and Maxfield, 1999). Figure 1 shows that shortly after internalization, the distribution of Tac-furin/ADA differs from that of Tac-furin; whereas the former localizes mostly to a central compartment (Figure 1B), the latter localizes to punctate, vesicular structures (Figure 1A). To analyze the pathway of Tac-furin/ADA en route to the TGN, cells were colabeled with Ax546-anti-Tac and DiI-LDL (5-min pulse, 10-min chase).

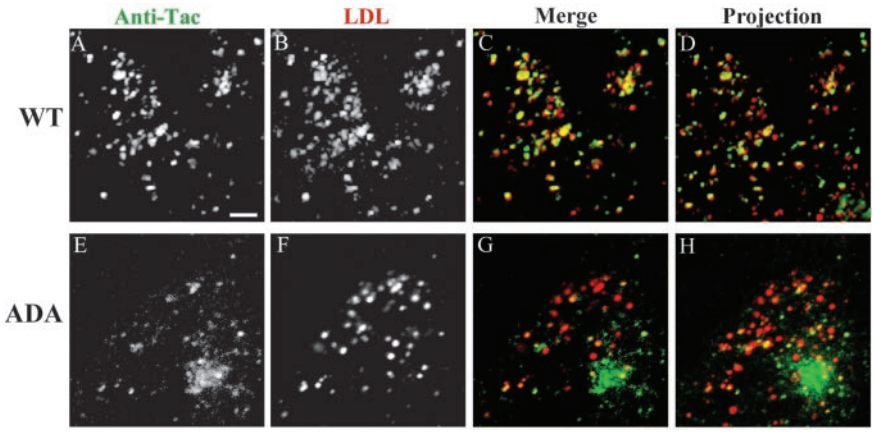

Figure 7. Internalized Tac-furin/ADA is delivered to the TGN without accumulation into late endosomes. Cells were incubated with Ax488-anti-Tac (A and E) and DiI-LDL (B and F) for 5 min, washed, chased for 10 min, and fixed. After 10-min chase, most of the LDL should be in late endosomes. (C and G) Merge of the anti-Tac signal (green) and the LDL signal (red). A–C and E–G show single confocal planes. A projection of successive confocal planes is shown in D and H. Colocalized areas range from orange to yellow. Bar, 10 μm.

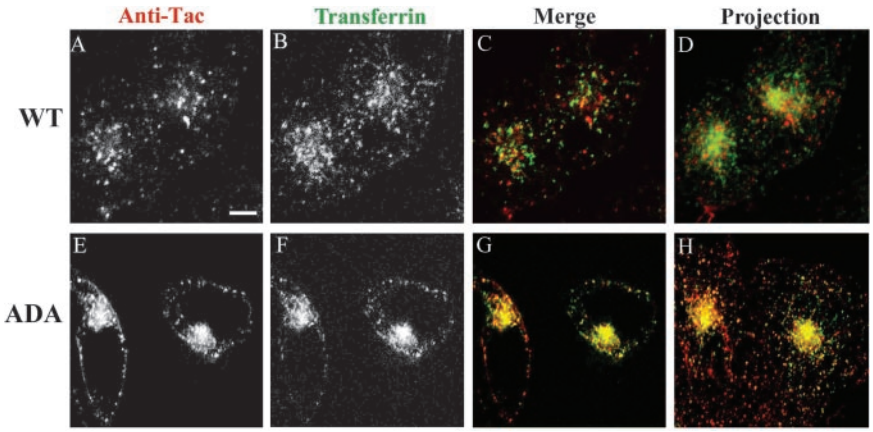

Figure 8. Internalized Tac-furin/ADA enters the ERC en route to the TGN. Cells were incubated with Ax546-anti-Tac (A and E) and with Ax488-transferrin (B and F) for 5 min, washed and chased for 1 min in the presence of Ax488–transferrin. Panels C and G show the merge of the anti-Tac signal (red) and the transferrin signal (green). Panels A–C and E–G show single confocal planes. A projection of successive confocal planes is shown in D and H. Colocalized areas range from orange to yellow. Bar, 10 μm.

Corroborating previous observations (Mallet and Maxfield, 1999), the majority of Tac-furin colocalizes with internalized DiI-LDL (Figure 7, A–D). In contrast, little colocalization is observed between DiI-LDL and Tac-furin/ADA (Figure 7, E–H), indicating that most of this construct is delivered to the TGN without significant accumulation into late endosomes. Similar results were obtained by colabeling WT and ADA mutant cell lines with anti-Tac and fluorescent dextran over a similar time course (our unpublished data).

To evaluate whether Tac-furin/ADA transits through the ERC en route to the TGN, cells were incubated for 5 min with Ax488-transferrin and Ax546-anti-Tac and chased for 1 min in the continuous presence of transferrin to label the recycling pathway. As reported previously (Hopkins and Trowbridge, 1983; Yamashiro *et al*., 1984), transferrin is detected primarily in the pericentriolar ERC and also in peripheral sorting endosomes. Tac-furin is present in an exclusively punctate distribution that does not colocalize with pericentriolar transferrin in the ERC (Figure 8, A–D). In contrast, Tac-furin/ADA displays a very good colocalization with this marker both at the ERC and in peripheral vesicles (Figure 8, E–H). These single plane images were focused on the Tac-furin labeling. As a consequence, although the transferrin-labeled ERC can be optimally visualized in cells expressing the mutant construct, this is not the case for cells expressing the WT construct because there is little Tac-furin in the ERC. A better appreciation of the overall transferrin staining can be observed in D and H, which show a projection of confocal planes. After a 15-min chase, Tac-furin/ADA starts to segregate from the ERC into a juxtanuclear structure that surrounds, but does not overlap, the ERC (Figure 9, E–H). Tac-furin presents a similar distribution at this time point (Figure 9, A–D). In both cases, the juxtanuclear structure was identified as TGN by using the marker TGN38 (our unpublished data).

To further characterize the transport of Tac-furin/ADA to the TGN, a triple labeling experiment was performed (Figure 10). Cells were pulsed with Ax488-transferrin and Ax546-anti-Tac for 5 min and chased for 10 min in the continuous presence of transferrin. Cells were then fixed, permeabilized, and labeled with anti-TGN38. At this time point, most of Tac-furin/ADA was found to colocalize with transferrin in the ERC (Figure 10D), whereas little colocalization with TGN38 was detected (Figure 10E). A small portion of the mutant construct does not overlap with TF or TGN38 (Figure 10F), suggesting that part of Tac-furin/ADA might be present in a compartment close to but different from the ERC, en route to the TGN. In contrast with the mutant construct, Tac-furin presents a punctate staining pattern that does not overlap with transferrin in the ERC.

The differential distribution of the Tac-furin/ADA construct reported above was corroborated by two series of experiments. In the first series, cells were coincubated with Ax-488 anti-Tac and HRP-Tf for 5 min, chased for 10 min in the presence of HRP-Tf, fixed, and treated with hydrogen peroxide and DAB. Whereas only 20% of the fluorescence was quenched in WT cells, mutant cells showed 72% quenching (Table 1). In the second series of experiments, late endosomes were labeled with HRP by preincubating the endocytic marker with the cells for 15 min, washing, pulsing

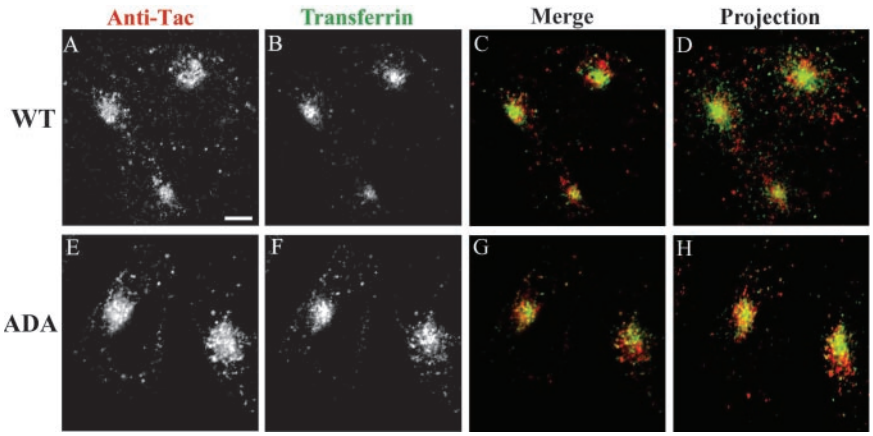

Figure 9. Internalized Tac-furin/ADA starts to segregate from the ERC into the TGN as early as 15 min after being internalized. Cells were incubated with Ax546-anti-Tac (A and E) and Ax488–transferrin (B and F) for 5 min, washed, and chased for 10 min in the presence of Ax488-transferrin. C and G show the merge of the anti-Tac signal (red) and the transferrin signal (green). A–C and E–G show single confocal planes. A projection of successive confocal planes is shown in D and H. Colocalized areas range from orange to yellow. Bar, 10 μm.

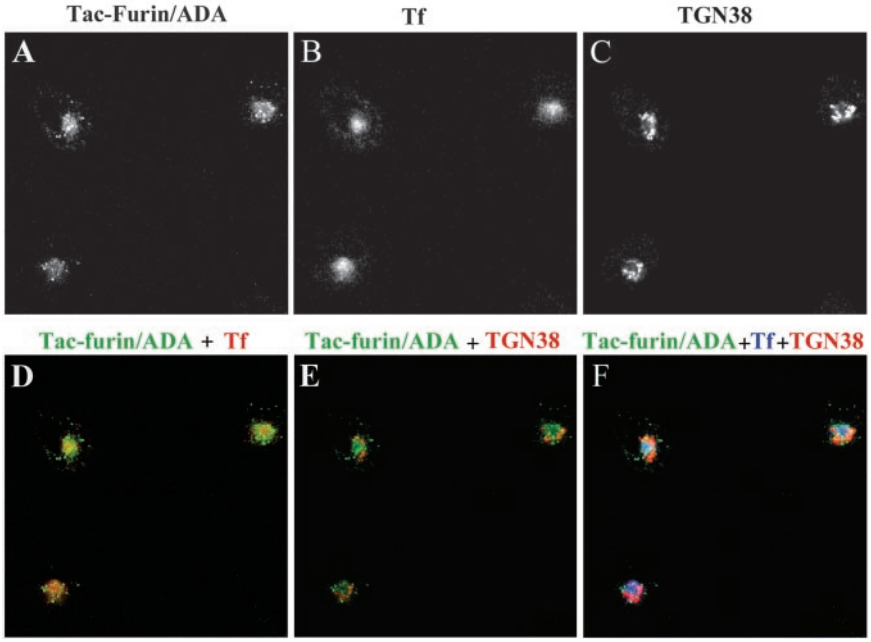

Figure 10. Most of Tac-furin/ADA localizes to the ERC after 10 min of being internalized. Cells were incubated with Ax488-anti-Tac (A) and Ax633-transferrin (Tf, B) for 5 min, washed and chased for 10 min in the presence of Ax633–transferrin. Cells were then fixed, permeabilized, and labeled with polyclonal antibodies against TGN-38, followed by Cy3-anti rabbit antibodies (C). (D) Merge of the anti-Tac signal (green) and the transferrin signal (red). (E) Merge of the anti-Tac signal (green) and the TGN38 signal (red). (F) Merge of the anti-Tac signal (green), the transferrin signal (blue) and the TGN38 signal (red). Single confocal planes are shown. Bar, 10 μm.

for 5 min with Ax488-Tf, and finally chasing for 10 min. In this case 64% of the fluorescence of WT cells was quenched, but only 15% of the fluorescence of cells expressing the mutant construct was quenched (Table 1). These results confirm that Tac-furin/ADA is targeted to the TGN through the ERC, without initial delivery into late endosomes.

Recycling of Tac-Furin/ADA to the Cell Surface after Internalization and at Steady State

Because internalized Tac-furin/ADA enters the ERC, we examined whether a fraction of it is returned to the cell surface as was observed for Tac-TGN38 (Ghosh *et al*., 1998). Cells were pulsed with Ax488-anti-Tac antibodies for 5 min, followed by incubation in the presence of anti-Ax488 quenching antibodies for various times. We determined that the anti-Ax488 antibodies quench Ax488-anti-Tac fluorescence by ~80% upon binding. At the concentration used, essentially no anti-Ax488 antibody reached either the ERC or the TGN in the absence of Ax488-anti-Tac, as observed by labeling with secondary antibodies (our unpublished data). Because fluorescence quenching requires a stoichiometric interaction of anti-Ax488 with Ax488-anti-Tac, a decrease in fluorescence can be attributed mainly to the Ax488-anti-Tac that reaches the plasma membrane being quenched by the anti-Ax488 antibodies present in the extracellular medium. Both cell lines present an initial decrease of fluorescence intensity, which represents the quenching of the cell surface fluorescence. After this initial drop, however, the fluorescence intensity of cells expressing Tac-furin remains constant throughout the chase (Figure 11 A, diamonds), confirming that little recycling of the WT construct takes place after a short filling pulse (Mallet and Maxfield, 1999). In contrast, the fluorescence intensity of cells expressing Tac-furin/ADA show a loss of fluorescence over time (Figure 11 A, squares), indicating that a portion of the mutant construct recycles back to the plasma membrane with each cycle of endocytosis.

Recycling of Tac-furin/ADA from inside of the cell to the plasma membrane at steady state was also investigated. Cells were incubated with Ax488-anti-Tac for 30 min, washed and chased for 2 h, to achieve a steady-state distribution. After this, further incubations for various times in the presence of the quenching antibody anti-Ax488 were performed. Cells expressing Tac-furin exhibit a gradual decrease of fluorescence intensity with time (Figure 11 B, diamonds), confirming the slow net rate of return described by Mallet and Maxfield (1999). Tac-furin/ADA–expressing cells show an even slower, very slight decrease of fluorescence intensity with time (Figure 11 B, squares), indicating that very little of this construct returns to the plasma membrane.

The overall degradation of Tac-furin and Tac-furin/ADA was determined by immunoprecipitation of ^{35}S-labeled proteins by using anti-Tac antibody, SDS-PAGE, and autoradiography. Both the WT and mutant constructs have a half-life of ~5 h.

DISCUSSION

Previous work showed that CHO cells have distinct mechanisms for endocytic transport of chimeric TGN transmembrane proteins Tac-TGN38 and Tac-furin, to the TGN. Although TGN targeting of Tac-TGN38 is mediated by the ERC, Tac-furin reaches the TGN via late endosomes, without traversing the recycling pathway. Although Tac-TGN38 is removed from the recycling pathway and delivered to the TGN in an iterative manner, Tac-furin is segregated from late endosomes into this organelle by a more efficient, single-pass mechanism (Ghosh *et al*., 1998; Mallet and Maxfield, 1999).

In the present work, we further analyzed the intracellular trafficking of furin, assessing the relevance of the serine phosphorylation sites at the cytoplasmic acidic cluster in the different steps of its trafficking. In agreement with previous reports (Schafer *et al*., 1995), we found that substitution of the phosphorylatable serines by alanines does not prevent internalization or TGN targeting of the mutant constructs. However, these mutations interfere with the postendocytic trafficking of the endoprotease. Instead of being retained in sorting endosomes, as seen with the WT, the mutant con-

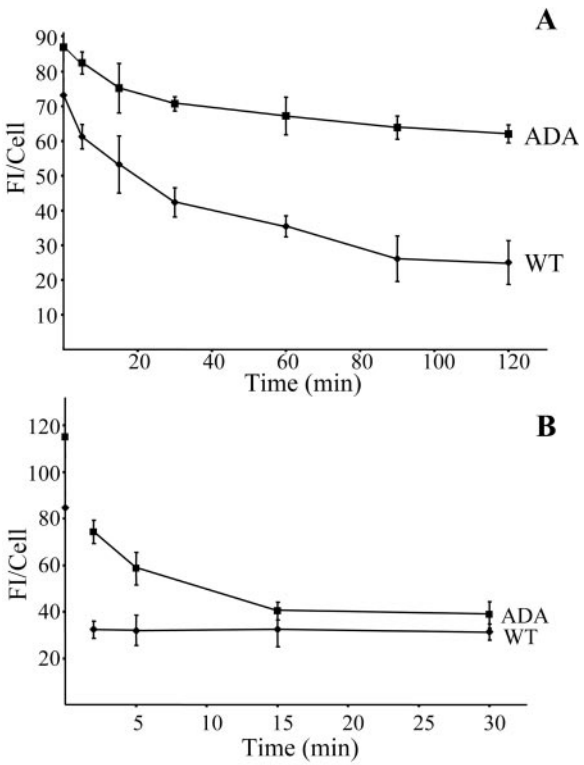

Figure 11. Postendocytic and steady-state retrieval of Tac-furin/ADA back to the plasma membrane after internalization. (A) A portion of Tac-furin/ADA is retrieved back to the plasma membrane after internalization. Cells were incubated with Ax488–anti-Tac for 5 min, washed and chased for 2, 5, 15, and 30 min in the presence of the quenching antibody anti-Ax488. (B) Sorting of Tac-furin/ADA from the TGN back to the plasma membrane at steady state is inhibited. Cells were incubated with Ax488–anti-Tac for 15 min, washed and chased for 2 h. Labeled cells were further incubated in the presence of anti-Ax488 for 5, 15, 30, 60, 90, and 120 min. In both sets of experiments, cell-associated fluorescence was quantified as described in MATERIALS AND METHODS. Data points represent the means of two independent experiments. Error bars indicate SEM.

struct is rapidly removed from sorting endosomes and passes through the ERC en route to the TGN. These results suggest that serine phosphorylation acts as an active sorting signal that causes retention of Tac-furin in the sorting endosomes and prevents its export to the ERC. The ability of Tac-furin/ADA to be delivered from the ERC to the TGN suggests that this construct has a second sequence that mediates selective removal of the protease from the recycling route and targeting to the TGN. Sequence analysis of the cytoplasmic domain of furin does not show similarity with other identified intracellular sorting signals, including SDYQRL, a sequence involved in TGN38 sorting (Bosshart *et al*., 1994). This ERC-to-TGN targeting signal of furin remains to be identified.

The alternate route taken by Tac-furin/ADA into the TGN, however, does not account for its steady-state distribution, characterized by a significant accumulation of the mutant construct in late endosomes. As shown by our photobleaching recovery experiments, Tac-furin/ADA returns to the TGN from late endosomes much more slowly than the WT Tac-furin, and this would account for the major features of the altered steady-state distribution. This is in agreement with a previous study (Wan *et al*., 1998), which showed that return of furin to the TGN from late endosomes depends on binding of PACS-1 to phosphorylated serines in AtT-20 cells. That study also reported that delivery from the TGN to late endosomes is independent of PACS-1 binding, which is consistent with our finding that Tac-furin/ADA is delivered to late endosomes after passing through the TGN.

Our data supports previous results from biochemical studies that showed that the phosphorylation state of furin is a major regulator of its trafficking (Jones *et al*., 1995; Molloy *et al*., 1998). Using various types of kinetic experiments based on intracellular localizations, we were able to dissect in detail the different steps of transport and obtain additional data that suggest a modification of the model of furin transport proposed earlier (Molloy *et al*., 1999). The major difference is in the early steps after furin internalization. In the previous model, it was proposed that after internalization phosphorylated furin binds to PACS-1 and is recycled back to the plasma membrane. In contrast, we found that mutation of the key serines to alanines leads to rapid exit of Tac-furin/ADA from sorting endosomes and delivery to the ERC. In fact, the phosphorylatable serines are required for retention of Tac-furin in sorting endosomes. A significant fraction of Tac-furin/ADA is recycled to the cell surface from the ERC, and some is delivered to the TGN.

Although the ADA mutation causes increased recycling from early endosomes to the cell surface, it decreases overall recycling to the cell surface. This is due to the dramatically slowed exit of Tac-furin/ADA from the late endosomes and delivery back to the TGN. This latter effect predominates over the changes in the early endosomal recycling because most of the Tac-furin is in the TGN-late endosomes recycling loop at steady state. The incomplete retrieval from late endosomes to the TGN (Figure 11A) indicates that a portion of the ADA construct becomes trapped in late endosomes and would eventually get degraded. The overall turnover rate of the Tac-furin and the Tac-furin/ADA is similar with a $t_{1/2}$ of ~5 h. This apparently reflects a balance of two counteracting effects: the Tac-furin is delivered to late endosomes from the plasma membrane more slowly, but once in late endosomes it leaves more slowly. A modified model of furin trafficking is shown in Figure 12. Interactions with several proteins, including PACS-1 (Wan *et al*., 1998), actin-binding protein of 280 kDa (Liu *et al*., 1997), and PP2A (Molloy *et al*., 1998), have been proposed to play a role in furin trafficking, especially in the late endosome-TGN loop. Further work will be required to identify the proteins required for proper sorting in the early endosomal system.

Recent studies performed in our laboratory addressed the intracellular trafficking of a chimeric form of the CI-MPR after endocytosis in CHO cells (Lin *et al*., 2003). These studies showed that, in contrast to furin, the endocytosed receptor achieves its steady-state distribution by transiting through the ERC and does not colocalize with late endosomal markers until after its passage through the pericentriolar region. Further differences in the transport of the CI-MPR and furin have been reported. Whereas retrieval of the receptor from late endosomes back to the TGN requires binding of tail-interacting protein of 47 kDa (TIP47) to its cytoplasmic domain (Díaz and Pfeffer, 1998), no interaction was detected between this cargo-binding protein and furin or phosphofurin (Krise *et al*., 2000). On the other hand, transport of the CI-MPR and furin also present similarities, such as the interaction of the acidic clusters of their cytoplasmic domains with PACS-1 in a phosphorylation-dependent manner (Wan *et al*., 1998). Overall, these observations indicate that there are similarities and differences in the trafficking of furin and the CI-MPR both in terms of their passage through organelles and their use of sorting proteins. Given that only a

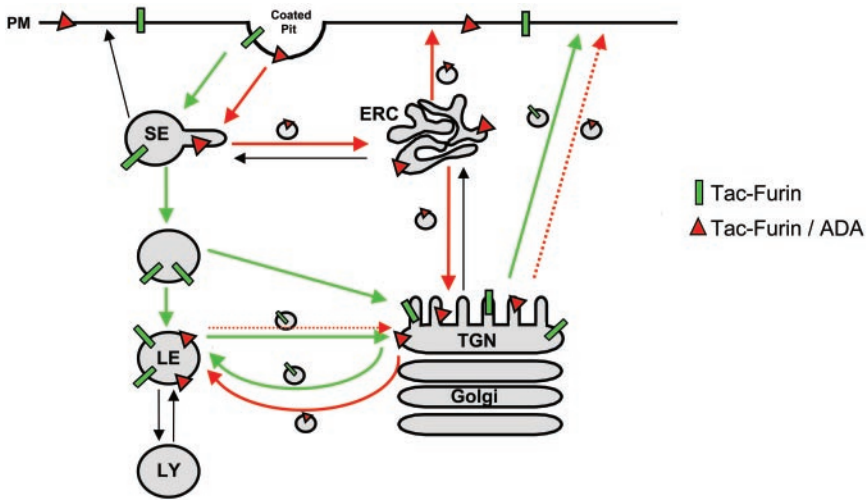

Figure 12. Model for the transport of Tac-furin and the mutant construct Tac-furin/ADA. Both constructs are internalized from the plasma membrane and initially enter sorting endosomes (SE). Tac-furin is then retained in the sorting endosomes as they mature into late endosomes (LE). Shortly after the endosomes lose the characteristics of sorting endosomes, Tac-furin is delivered from the maturing endosomes into the TGN. This may occur in the maturing endosome/endosome carrier vesicle (Gruenberg and Maxfield, 1995). In contrast, Tac-furin/ADA is removed rapidly from sorting endosomes and transported to the ERC. Although a portion of the mutant construct is recycled back to the cell surface, the rest is delivered to the TGN as is the case for TGN38. Black arrows represent steps of protein traffic that exist, but are not followed by Tac-furin nor Tac-furin/ADA. The stippled TGN-PM arrow represents decreased retrieval of Tac-furin/ADA from the TGN to the PM.

small percentage of total cell surface proteins are transported back to the Golgi complex, it might have been expected that this subset of proteins would share a common route of intracellular transport. However, plentiful evidence (Bos *et al*., 1993; Ghosh *et al*., 1998; Mallet and Maxfield, 1999; Krise *et al*., 2000; Lin *et al*., 2003) supports the existence of multiple pathways for transport to the TGN. Selective sorting into different types of vesicles might be mediated by specific interactions with different adaptor complexes and/or other sorting proteins. Further work will be required to characterize the molecular components of each step of these pathways.

The Tac-furin/ADA construct studied in this article initially traffics similarly to TGN38 and the CI-MPR. All these proteins exit the sorting endosomes rapidly and are delivered to the ERC. A fraction of each of the proteins is then diverted from the recycling route to the TGN. Because the wild-type furin does not enter the ERC in significant amounts, the delivery of the Tac-furin/ADA from the ERC to the TGN reveals a redundant sorting pathway that ensures delivery of furin to the TGN. Once in the TGN, Tac-furin, Tac-furin/ADA, and the CI-MPR are delivered to late endosomes. Retrieval from the late endosomes to the TGN is inhibited by loss of the phosphorylatable serines, consistent with previous studies implicating a role for PACS-1 in this retrieval (Wan *et al*., 1998). The retention of furin in sorting endosomes requires phosphorylatable serines, which implicates these residues in a different type of sorting process. That is, they promote retention in sorting endosomes but export from late endosomes. This type of behavior could account for the rapid export of furin from endosomes shortly after they mature from sorting endosomes into late endosomes (Mallet and Maxfield, 1999).

ACKNOWLEDGMENTS

We thank George Banting for the anti-TGN38 antibody, Timothy McGraw for critical reading of the manuscript, and Enrique Rodriguez-Boulan, Anne Muesch, and David Cohen for sharing advice, technical expertise, and reagents in the lifetime measurements. This work was supported by National Institutes of Health grant DK-27083 (to F.R.M.). F.B.S. was supported by a Norman and Rosita Winston Foundation postdoctoral fellowship in Biomedical Sciences.

REFERENCES

Bos, K., Wraight, C., and Stanley, K.K. (1993). TGN38 is maintained in the trans-Golgi network by a tyrosine-containing motif in the cytoplasmic domain. EMBO J. *12*, 2219–2228.

Bosshart, H., J. Humphrey, E. Deignan, J. Davidson, J. Drazba, L. Yuan, V. Oorschot, P. J. Peters, and J. S. Bonifacino. (1994). The cytoplasmic domain mediates localization of furin to the trans-Golgi network en route to the endosomal/lysosomal system. J. Cell Biol. *126*, 1157–1172.

Díaz, E., and Pfeffer, S.R. (1998). TIP *47*, a cargo selection device for mannose 6-phosphate receptor trafficking. Cell *93*, 433–443.

Duncan, J.R., and Kornfeld, S. (1988). Intracellular movement of two mannose 6-phosphate receptors: return to the Golgi apparatus. J. Cell Biol. *106*, 617–628.

Ghosh, R.N., Mallet, W.G., Soe, T.T., McGraw, T.E., and Maxfield, F.R. (1998). An endocytosed TGN38 chimeric protein is delivered to the TGN after trafficking through the endocytic recycling compartment in CHO cells. J. Cell Biol. *142*, 923–936.

Gruenberg, J., and Maxfield, F.R. (1995). Membrane transport in the endocytic pathway. Curr. Opin. Cell Biol. *7*, 552–563.

Gu, F., Crump, C.M., and G. Thomas. (2001). Trans-Golgi network sorting. Cell. Mol. Life Sci. *58*, 1067–1084.

Hopkins, C.R., and Trowbridge, I.S. (1983). Internalization and processing of transferrin and the transferrin receptor in human carcinoma A431 cells. J. Cell Biol. *97*, 508–521.

Humphrey, J.S., Peters, P.J., Yuan, L.C., and Bonifacino, J.S. (1993). Localization of TGN38 to the trans-Golgi network: involvement of a cytoplasmic tyrosine-containing sequence. J. Cell Biol. *120*, 1123–1135.

Johnson, A.O., Ghosh, R.N., Dunn, K.W., Garippa, R., Park, J., Mayor, S., Maxfield, F.R., and McGraw, T.E. (1996). Transferrin receptor containing the SDYQRL motif of TGN38 causes a reorganization of the recycling compartment but is not targeted to the TGN. J. Cell Biol. *135*, 1749–1762.

Jones, B.G., Thomas, L., Molloy, S.S., Thulin, C.D., Fry, M.D., Walsh, K.A., and Thomas, G. (1995). Intracellular trafficking of furin is modulated by the phosphorylation state of a casein kinase II site in its cytoplasmic tail. EMBO J. *14*, 5869–5883.

Jones, S.M., Crosby, J.R., Salamero, J., and Howell, K.E. (1993). A cytosolic complex of p62 and rab6 associates with TGN38/41 and is involved in budding of exocytic vesicles from the trans-Golgi network. J. Cell Biol. *122*, 775–788.

Krise, J.P., Sincock, P.M., Orsel, J.G., and Pfeffer, S.R. (2000). Quantitative analysis of TIP47-receptor cytoplasmic domain interactions: implications for endosome-to-trans Golgi network trafficking. J. Biol. Chem. *275*, 25188–25193.

Lin S. X., Mallet W.G., Huang A.Y., and. Maxfield F.R. (2003). Endocytosed Cation-Independent Mannose 6-Phosphate Receptor Traffics via the Endocytic Recycling Compartment en Route to the trans-Golgi Network and a Sub-Population of Late Endosomes. Mol. Biol. Cell *15*, 721–733.

Liu, G., Thomas, L., Warren, R.A., Enns, C.A., Cunningham, C.C., Hartwig, J.H., and Thomas, G. (1997). Cytoskeletal protein ABP-280 directs the intracellular trafficking of furin and modulates proprotein processing in the endocytic pathway. J. Cell Biol. *139*, 1719–1733.

Mayor, S., Sabharanjak, S., and Maxfield, F.R. (1998). Cholesterol-dependent retention of GPI-anchored proteins in endosomes. EMBO J. *17*, 4626–4638.

Mallet, W.G., and Maxfield, F.R. (1999). Chimeric forms of furin and TGN38 are transported with the plasma membrane in the trans-Golgi network via distinct endosomal pathways. J. Cell Biol. *146*, 345–359.

Maxfield, F.R., and McGraw, T.E. (2004). Endocytic recycling. Nat. Rev. Mol. Cell. Biol. *5*, 121–132

McGraw, T.E., Greenfield, L., and Maxfield, F.R. (1987). Functional expression of the human transferrin receptor cDNA in Chinese hamster ovary cells deficient in endogenous transferrin receptor. J. Cell Biol. *105*, 207–214.

Milgram, S.L., Mains, R.E., and Eipper, B.A. (1993). COOH-terminal signals mediate the trafficking of a peptide processing enzyme in endocrine cells. J. Cell Biol. *121*, 23–36.

Molloy, S.S., Anderson, E.D., Jean, F., and Thomas, G. (1999). Bi-cycling the furin pathway: from TGN localization to pathogen activation and embryogenesis. Trends Cell Biol. *9*, 28–35.

Molloy, S.S., Thomas, L., Kamibayashi, C., Mumby, M.C., and Thomas, G. (1998). Regulation of endosome sorting by a specific PP2A isoform. J. Cell Biol. *142*, 1399–1411.

Molloy, S.S., Thomas, L., VanSlyke, J.K., Stenberg, P.E., and Thomas, G. (1994). Intracellular trafficking and activation of the furin proprotein convertase: localization to the TGN and recycling from the cell surface. EMBO J. *13*, 18–33.

Mukherjee, S., Ghosh, R.N., and Maxfield, F.R. (1997). Endocytosis. Physiol. Rev. *77*, 759–803.

Pitas, R.E., Innerarity, T.L., Weinstein, J.N., and Mahley, R.W. (1981). Acetoacetylated lipoproteins used to distinguish fibroblasts from macrophages in vitro by fluorescence microscopy. Arteriosclerosis *1*, 177–185.

Reaves, B., Horn, M., and Banting, G. (1993). TGN38/41 recycles between the cell surface and the TGN: brefeldin A affects its rate of return to the TGN. Mol. Biol. Cell *4*, 93–105.

Schafer, W., Stroh, A., Berghofer, S., Seiler, J., Vey, M., Kruse, M.L., Kern, H.F., Klenk, H.D., and Garten, W. (1995). Two independent targeting signals in the cytoplasmic domain determine trans-Golgi network localization and endosomal trafficking of the proprotein convertase furin. EMBO J. *14*, 2424–2435.

Takahashi, S., Nakagawa, T., Banno, T., Watanabe, T., Murakami, K., and Nakayama, K. (1995). Localization of furin to the trans-Golgi network and recycling from the cell surface involves Ser and Tyr residues within the cytoplasmic domain. J. Biol. Chem. *270*, 28397–28401.

Varlamov, O., Eng, F.J., Novikova, E.G., and Fricker, L.D. (1999). Localization of metallocarboxypeptidase D in AtT-20 cells. Potential role in prohormone processing. J. Biol. Chem. *274*, 14759–14767.

Voorhees, P., Deignan, E., van Donselaar, E., Humphrey, J., Marks, M.S., Peters, P.J., and Bonifacino, J.S. (1995). An acidic sequence within the cytoplasmic domain of furin functions as a determinant of trans-Golgi network localization and internalization from the cell surface. EMBO J. *14*, 4961–4975.

Wan, L., Molloy, S.S., Thomas, L., Liu, G., Xiang, Y., Rybak, S.L., and Thomas, G. (1998). PACS-1 defines a novel gene family of cytosolic sorting proteins required for trans-Golgi network localization. Cell *94*, 205–216.

Yamashiro, D.J., Tycko, B., Fluss, S.R., and Maxfield, F.R. (1984). Segregation of transferrin to a mildly acidic (pH 6.5) para-Golgi compartment in the recycling pathway. Cell *37*, 789–800.